M&C 2017 - International Conference on Mathematics & Computational Methods Applied to Nuclear Science & Engineering, Jeju, Korea, April 16-20, 2017, on USB (2017)

Improved Correlated Sampling For Iteratively Coupled PDE/Monte-Carlo Methods Used In Plasma Edge Simulations

M. Baeten,* B. Mortier,* M. Baelmans,† G. Samaey*

*KU Leuven, Department of Computer Science, Celestijnenlaan 200A, 3001 Leuven, Belgium
†KU Leuven, Department of Mechanical Engineering, Celestijnenlaan 300A, 3001 Leuven, Belgium
matthias.baeten@kuleuven.be

Abstract - *The plasma edge of nuclear fusion devices is typically analyzed by means of an iteratively coupled Finite Volume (FV) / Monte Carlo (MC) simulation. At present, this is performed using randomly reseeded MC calculations in each iteration, as convergence problems arise with correlated sampling. In this paper, we analyze the convergence problems associated with correlated sampling for a simplified 1D case. We show that discontinuities in the discretized plasma profile play a critical role. We provide an adequate linear interpolation, both in the MC procedure and in the implementation of the reflecting boundary conditions at the target, to eliminate the convergence problems.*

I. INTRODUCTION

At present, numerical simulations of the plasma and neutral transport in the plasma edge and divertor region of nuclear fusion devices serve to interpret experimental observations and to design next generation reactors such as ITER and DEMO [1]. To this end, the B2-EIRENE code [2] is used worldwide. The plasma is modeled with PDEs (continuum approximation), while the neutral particles are described by a kinetic equation. These two sets of equations are strongly coupled because of mutual interactions between plasma and neutral particles. On the one hand, these interactions give rise to source terms in the fluid equations. On the other hand, the cross-sections and collision kernels in the kinetic equation, as well as the sources for the neutral particles, strongly depend on plasma quantities. An FV method for the plasma equations and an MC simulation of the neutral particles are iteratively coupled and solved alternately until convergence is attained. The used iterative method is a pseudo-transient continuation method.

One way of coupling the FV and MC code is the correlated sampling technique, where the same pseudorandom numbers in the MC code are used at every iteration. With correlated sampling, the computed solution is still random, as it depends on the chosen random numbers in the MC part of the simulation. However, the procedure is able to let both the plasma quantities and the neutral particle trajectories converge to a fixed state. This way, the residuals of the discretized plasma equations can decrease to a certain level for which the convergence error[1] can be neglected in comparison with the discretization error and/or statistical[2] error. While correlated sampling is an appealing and conceptually simple technique, it turns out to be a big challenge to make it work in practice. Nowadays with the B2-EIRENE code [1, 2], convergence of the residual up to such an acceptable magnitude can only be achieved for a small fraction of potential seeds.

In this paper, we study in detail the convergence problems of correlated sampling in a simplified 1D simulation code. We start by briefly describing the simplified coupled continuum-kinetic model for the plasma and neutral transport in our 1D setting. The simulation results obtained with this 1D model can not be used for practical purposes, but we expect that the causes of the convergence problems for our 1D code and for the B2-EIRENE code are the same. Next, we describe the coupled FV/MC code for the numerical simulation of the 1D model and illustrate the convergence problems of the correlated sampling technique. We then turn to an analysis of the causes. It turns out that from the 100 initial test runs we did, 31 do not converge as a consequence of the discretized plasma representation and 2 due to the impact of boundary conditions. We show how to avoid these problems and perform an additional 150 runs to increase our confidence that we eliminated all convergence issues.

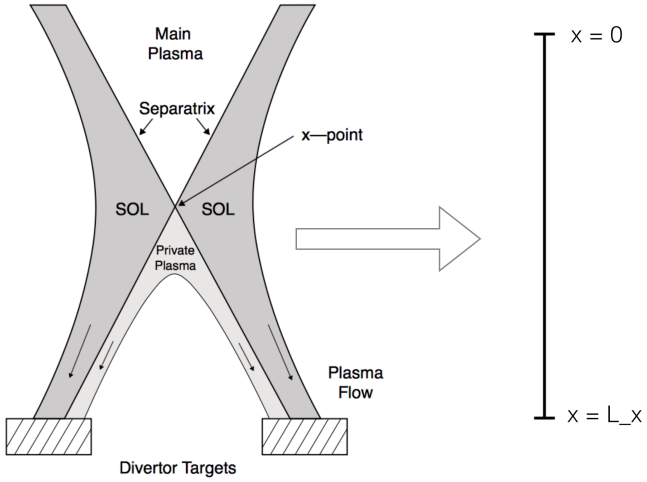

Fig. 1: Reduction of the 2D plasma edge domain (poloidal cross section) used in the B2-EIRENE code to the interval $[0, L_x]$ (1D domain). This figure originates from ref. [3].

II. 1D COUPLED CONTINUUM-KINETIC MODEL

When simulating the plasma edge and divertor region in a tokamak device, a stationary flow and toroidal symmetry are often assumed. The plasma and neutral transport are then simulated in a poloidal cross section of the tokamak. This

[1] We define the convergence error as the error on the computed solution due to a non-zero residual of the nonlinear discretized plasma equations.

[2] The statistical error is the error on the computed solution due to the use of a finite number of samples for the MC simulation of the neutral particles.

two-dimensional domain is shown in figure 1. The 2D plasma-neutral model [4, 5] and the corresponding B2-EIRENE simulation code [1, 2, 5] that are used in practice, are rather complex and computationally demanding. Because we only intend to study the numerical problems with correlated sampling, we will use, instead of the 2D plasma-neutral model, a simplified one-dimensional model for which the convergence problems with correlated sampling are still present. We expect that the solution we propose here should also work in the 2D case.

In this section we describe the 1D model. The domain is the interval $[0, L_x]$ where $x = 0$ represents the upstream position and $x = L_x$ represents the target. This is graphically shown in figure 1. In our numerical simulations, we use a domain length $L_x = 1.069$m.

The transport of the plasma particles is described by the Braginskii equations [6]. A series of simplifications are performed in our 1D model. Besides a stationary plasma flow, we assume that the electron density n_e is equal to the ion density n_i (quasi-neutrality), that the magnetic field is constant and that electric currents equal zero (ambipolarity). We also let the temperature profiles T_i and T_e of the ions and electrons respectively be known in advance to eliminate the energy equation. What remains are the continuity equation and the momentum equation for the ions:

$$\boldsymbol{S}_{n_i} - \frac{\partial(n_i b_x u_p)}{\partial x} = 0\,, \tag{1}$$

$$\boldsymbol{S}_{mo} - b_x \frac{\partial p}{\partial x} - m_i \frac{\partial(n_i b_x u_p^2)}{\partial x} + \frac{\partial}{\partial x}\left(b_x^2 \eta_p \frac{\partial u_p}{\partial x}\right) = 0\,. \tag{2}$$

The parallel velocity u_p represents the velocity of the ions parallel to the magnetic field. The symbol b_x represents the magnetic pitch and is the ratio between the magnetic field component in the 1D domain and the total magnetic field. In this way the product $b_x u_p$ represents the velocity component of the plasma in our 1D domain. The pitch profile is assumed to be known in advance. The mass source $\boldsymbol{S}_{n_i}$ and momentum source $\boldsymbol{S}_{mo}$ originates from interactions between ionized particles (plasma) and neutrally charged particles. The pressure p equals

$$p = n_i(x)T_i(x) + n_e(x)T_e(x)\,. \tag{3}$$

The parallel viscosity η_p and the sound speed c_s are defined as follows:

$$\eta_p(x) = 3.8\text{e}{-10} \cdot \left(\frac{T_i(x)}{40\text{eV}}\right)^{\frac{5}{2}}, \tag{4}$$

$$c_s(x) = \sqrt{\frac{T_i(x) + T_e(x)}{m_i}}\,, \tag{5}$$

where m_i is the ion mass of deuterium. The boundary conditions are the following:

$$n_i(0) = 10^{20} m^{-3}\,, \tag{6}$$

$$u_p(L_x) = c_s(L_x)\,, \tag{7}$$

$$\frac{\partial u_p}{\partial x}(0) = 0\,. \tag{8}$$

The plasma mainly flows into the direction of the divertor target ($x = L_x$). When the plasma particles hit the target, they become neutralized. These neutral particles flow into the plasma edge region where they interact with the plasma and eventually ionize again. In contrast to the plasma model, the neutral particle flow can not be well described with a continuum approximation. A more microscopic model is needed. Therefore kinetic equations are used instead of fluidum equations, such that their transport and the collisions can be described in an accurate way. In the B2-EIRENE code a multi species set of coupled nonlinear Boltzmann equations are solved [5] to simulate the stationary neutral particle flow. In our 1D model, we consider only one type of neutrals, described by a reduced linear Boltzmann equation where we assume that the neutral particles only interact with the plasma and not with each other. Two types of interactions are considered: ionization[3] and charge exchange[4]. The macroscopic cross sections for ionization and charge exchange are

$$\Sigma_{\text{ion}}(x, v) = \frac{R_{\text{ion}}(x)}{|v|} = \frac{n_e(x) K_{\text{ion}}}{|v|}, \tag{9}$$

$$\Sigma_{\text{cx}}(x, v) = \frac{R_{\text{cx}}(x)}{|v|} = \frac{n_i(x) K_{\text{cx}}}{|v|}\,, \tag{10}$$

where x and v represent the position and velocity of the neutral particle. The total cross section Σ_{tot}, respectively the total reaction rate R_{tot}, is equal to the sum of the two cross sections Σ_{ion} and Σ_{cx}, respectively two reaction rates R_{ion} and R_{cx}. The constants K_{ion} and K_{cx} are the rate coefficients for ionization and charge exchange. The Boltzmann equation characterizes the neutral distribution function $f_n(x, v)$ in phase space $[0, L_x] \times \mathbb{R}$ as follows:

$$v\,\frac{\partial f_n(x,v)}{\partial x} \;+\; \Sigma_{\text{tot}}(x,v)\,|v|\,f_n(x,v) \;=\; S(x,v) \;+ \int_{\mathbb{R}} \Sigma_{\text{tot}}(x,v')\,|v'|\,f_n(x,v')\,C(x,v' \to v)\,dv'\,. \tag{11}$$

The collision kernel $C(x, v' \to v)$ represents the probability that the initial velocity v' of a neutral particle changes into a velocity v due to a collision with a plasma particle at position x. Because a neutral particle dissapears after it gets ionized, only the charge exchange cross section contributes to the collision kernel.

$$C(x, v' \to v) \;= \frac{R_{\text{cx}}(x)}{R_{\text{tot}}(x)} \sqrt{\frac{m_i}{4\pi T_i(x)}} \exp\left(- \frac{m_i}{4T_i(x)} \Big(v - b_x(x) u_p(x)\Big)^2 \right) \tag{12}$$

The collision kernel contains a one-dimensional Maxwellian distribution. Hence the new velocity v after a charge exchange is normal distributed with mean $\mu(x) = b_x u_p$ and variance $\sigma^2(x) = 2T_i/m_i$. Notice in (12) that the new velocity v is

[3] A particle that initially has a neutral charge before the collision, gets ionized and belongs to the plasma from now on.

[4] After a charge exchange interaction, the neutral particle gets ionized and the plasma particle acquires a neutral charge. When simulating a charge exchange in the MC code, the initial neutral particle stays neutral and acquires a new velocity. An individual plasma particle is never simulated (continuum approximation).

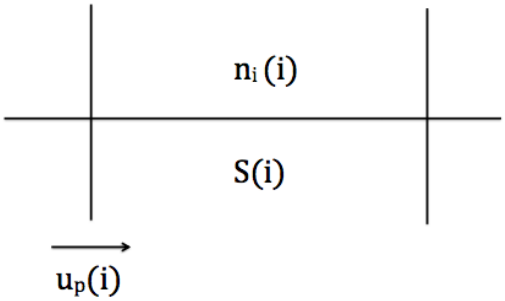

Fig. 2: Graphical representation of the staggered grid used for the plasma equations. This figure originates from ref. [7].

independent of the previous velocity v'. The source term in the kinetic equation represents the birth of neutral particles at the target (recycling) because of plasma-target interactions.

$$S(x,v) = R\, c_s(L_x)\, b_x(x)\, n_i(x)\, \delta(x-L_x)\, \delta\Big(\frac{v}{|v|}+1\Big), \quad (13)$$

The constant $R = 0.99$ is the recycling coefficient and δ is a Dirac delta function.

As seen above, the plasma quantities influence the neutral particle trajectories, where as the neutral particles generate source terms in the plasma equations (1) and (2). What remains is to define these sources in terms of the neutral state.

$$\boldsymbol{S}_{n_i}(x) = R_{\text{ion}}(x)\, n_n(x)\,, \quad (14)$$

$$\boldsymbol{S}_{mo}(x) = m_i\, n_n(x)\, \Big(R_{\text{tot}}(x)u_n(x) \;-\; R_{\text{cx}}(x)b_x(x)u_p(x)\Big), \quad (15)$$

where $n_n(x)$ and $u_n(x)$ are respectively the neutral density and poloidal neutral velocity at position x:

$$n_n(x) = \int_{\mathbb{R}} f_n(x,v)\, dv\,, \quad (16)$$

$$u_n(x) = \frac{1}{n_n(x)} \int_{\mathbb{R}} v f_n(x,v)\, dv\,, \quad (17)$$

In the B2-EIRENE code the coupled continuum-kinetic model for the plasma-neutral transport is simulated by coupling a Finite Volume (FV) method for the plasma equations with a Monte Carlo method for the neutral transport equation. In the next two sections the FV and MC method are elaborated.

III. FINITE VOLUMES FOR PLASMA EQUATIONS

Equations in fluid mechanics are usually discretized using an FV method because of its conservation properties. For the same reason, the FV method is also employed for the plasma equations (1) and (2) in the B2-EIRENE code. A staggered grid is used in which the plasma velocity u_p is defined at the cell faces. The ion density n_i, the pitch b_x, the temperatures T_i, T_e and the source terms $\boldsymbol{S}_{n_i}, \boldsymbol{S}_{mo}$ are all defined at the cell centers. This is graphically shown in figure 2. The ion density, pitch and temperatures are also stored at the two domain boundaries because of boundary conditions.

In the FV code for the 1D model, first order upwind schemes are employed. The resulting discretized plasma equations are a finite set of nonlinear equations that we will denote by $\boldsymbol{F}(\boldsymbol{\mu}, \boldsymbol{S}(\boldsymbol{\mu})) = \boldsymbol{0}$. The vector $\boldsymbol{\mu}$ contains all macroscopic plasma quantities at their discrete locations. Similarly, the vector[5] $\boldsymbol{S}(\boldsymbol{\mu})$ contains the source terms $\boldsymbol{S}_{n_i}$ and $\boldsymbol{S}_{mo}$ at the cell centers. The nonlinear system is solved using a pseudo-transient continuation procedure[6]. The idea behind it is to solve the related initial value problem below:

$$\frac{\mathrm{d}\boldsymbol{\mu}}{\mathrm{d}t} + \boldsymbol{F}(\boldsymbol{\mu}, \boldsymbol{S}(\boldsymbol{\mu})) = \boldsymbol{0}, \;\; \boldsymbol{\mu}(0) = \boldsymbol{\mu}_0\,, \quad (18)$$

where we select the initial plasma state $\boldsymbol{\mu}_0$ ourselves. A time integration method will be employed to iterate to the steady state solution (which is the solution of the nonlinear system). For pseudo-transient continuation, usually a first order Rosenbrock[7] method is used as time integrator [9]. With the plasma state $\boldsymbol{\mu}_k$ and the corresponding source terms $\boldsymbol{S}_k(\boldsymbol{\mu}_k)$ at iteration k, the plasma state $\boldsymbol{\mu}_{k+1}$ at the next iteration is then computed as follows:

$$\boldsymbol{\mu}_{k+1} = \boldsymbol{\mu}_k - \alpha \left(\frac{1}{\Delta t} I + \frac{\partial \boldsymbol{F}}{\partial \boldsymbol{\mu}}\Big(\boldsymbol{\mu}_k, \boldsymbol{S}_k(\boldsymbol{\mu}_k)\Big)\right)^{-1} \boldsymbol{F}\Big(\boldsymbol{\mu}_k, \boldsymbol{S}_k(\boldsymbol{\mu}_k)\Big), \quad (19)$$

where the dependence of $\boldsymbol{S}_k$ on $\boldsymbol{\mu}_k$ is ignored when deriving the analytical expression of the Jacobian matrix in (19). For stability, we use a relaxation factor $\alpha = 0.5$. At the start of every iteration k, the source terms $\boldsymbol{S}_k(\boldsymbol{\mu}_k)$ corresponding to the plasma state $\boldsymbol{\mu}_k$ have to be computed. Since the source terms depend also on the neutral density and neutral velocity (see equations (14) and (15)), the neutral transport equation (11) has to be solved at every iteration. The MC method used to compute the neutral quantities is elaborated in the next section.

IV. MONTE CARLO SIMULATION OF NEUTRAL TRANSPORT

In every iteration k of our pseudo-transient continuation procedure, the neutral quantities (density and velocity) corresponding to the current plasma state $\boldsymbol{\mu}_k$ have to be computed. The cross-sections (9), (10), collision kernel (12) and neutral source term (13) in the neutral transport equation (11) depend on the plasma state $\boldsymbol{\mu}_k$.

The high dimensionality of the kinetic equations in the 2D plasma-neutral model, makes a Monte Carlo method the only option to compute the neutral quantities within a reasonable CPU time. In our simplified 1D model, we also use an MC method to simulate the neutral transport, since the stochasticity introduced by the MC method is the main topic of our study. To estimate the neutral quantities, the MC method simulates a finite number of neutral particle trajectories in a non-analog way: every path starts with a statistical weight W of 1 and instead of letting the particle disappear after an ionization, the weight is multiplied after each interaction with the probability of surviving the interaction. I.e., the probability that the event was charge exchange, leading to a new particle velocity. When

[5] We write $\boldsymbol{S}$ as a function of $\boldsymbol{x}$ because the source terms depend on plasma quantities. This fact is ignored when discretizing the plasma equations.

[6] In the literature, this method is also known as false-time stepping or pseudo-time stepping.

[7] A more detailed elaboration of Rosenbrock methods and there convergence and stability properties can be found in ref. [8].

a particle hits the domain boundary, the weight is multiplied with the probability of non-absorption and then a reflection is simulated, by reversing the velocity. A particle is ionized or absorbed if its weight is below a certain threshold. A simulated trajectory $t \mapsto (X(t), W(t))$ can be described by the velocity-jump process defined below.

$$\begin{cases} X(t) = X(t_n) + v_n(t - t_n) & \text{for } t \in [t_n, t_{n+1}] \quad (20a) \\ W(t) = \dfrac{R_{\text{cx}}(X(t_n))}{R_{\text{tot}}(X(t_n))} W(t_{n-1}) & \text{for } t \in [t_n, t_{n+1}[\quad (20b) \\ (v_n)_{n\geq 1} \sim \mathcal{N}\Big(b_x\big(X(t_n)\big) \cdot u_p\big(X(t_n)\big), \dfrac{2T_i(X(t_n))}{m_i}\Big) & (20c) \\ \displaystyle\int_{t_n}^{t_{n+1}} R_{\text{tot}}\big(X(t)\big)\,\mathrm{d}t = \theta_n & (20d) \\ (\theta_n)_{n\geq 0} \sim \mathcal{E}(1) \text{ i.i.d.} & (20e) \end{cases}$$

For simplicity, we left the boundary conditions and the weight threshold, that determines when a particle is actually removed from the simulation, out of the velocity-jump description. Neutral particles arise at the target, so the initial conditions are $t_0 = 0$, $X(t_0) = L_x$, $W(t_0) = 1$ and $v_0 < 0$. The initial velocity v_0 is sampled from a truncated[8] Maxwellian distribution. The velocity v_n of a neutral particle changes after a collision at time t_n. Neutral velocities are sampled from a normal distribution with plasma dependent parameters, see (20c). Equations (20d) and (20e) express that the intercollision time $\tau = t_{n+1} - t_n$ is sampled from an exponential distribution with a position dependent rate. This rate is the total reaction rate $R_{\text{tot}}(x)$. The cumulative distribution function of the intercollision time τ is

$$F_c(\tau) = \int_0^\tau R_{\text{tot}}\big(X(t_n + u)\big) \exp\Big(-\int_0^u R_{\text{tot}}\big(X(t_n + t)\big)\,\mathrm{d}t\Big)\,\mathrm{d}u\,. \quad (21)$$

The plasma quantities in the kinetic neutral model are defined over the domain interval $[0, L_x]$, while the plasma quantities in the current iteration are only computed at discrete grid points. To overcome this issue, nearest-neighbor interpolation is used in the B2-EIRENE code. This means that the values of the plasma quantities at a certain position are approximated by their computed values at the center of the FV cell where the collision occurs. Nearest-neighbor interpolation leads to a piecewise constant plasma profile during the MC simulation. As we will show in subsequent sections, this discontinuous plasma profile causes the convergence problems with correlated sampling. The piecewise constant plasma profile makes the profile of the total reaction rate R_{tot} also piecewise constant, such that the cumulative density of τ, given by (21), can be worked out to obtain

$$F_c(\tau) = 1 - \prod_{j=0}^{J} \exp\Big(-R_{\text{tot}}^j \Delta\tau_j\Big) \quad \text{with} \quad \sum_{j=0}^{J} \Delta\tau_j = \tau\,. \quad (22)$$

The number of cells that the particle encountered during the intercollision phase is presented with the symbol J. The total rate and the time spent in the j-th encountered cell during the intercollision phase are denoted by R_{tot}^j and $\Delta\tau_j$ respectively. The intercollision time τ is sampled by using equation (22) and the probability integral transform.

By simulating a finite number of weighted trajectories, MC estimates of the neutral density n_n and neutral velocity u_n are obtained in every FV cell with the use of the track-length estimator. For a comprehensive explanation of how the track-length estimator works, we refer to Ref. [10].

V. COUPLED ITERATION AND LACK OF CONVERGENCE

The FV code for the plasma transport and the MC code for the neutral transport are iteratively coupled. This coupling can be done in different ways. One way of coupling is the correlated sampling technique, where the same pseudorandom numbers are used in the MC code at every iteration. The goal of correlated sampling is to let both the plasma quantities and the neutral quantities (neutral particle trajectories) converge to a fixed state, such that the residual of the discretized plasma equations can decrease to a desired magnitude. Currently when using the B2-EIRENE code with correlated sampling, the residual stagnates at a level that is too large causing the correlated sampling technique to loose its main advantage.

In this paper, we attempt to figure out why with correlated sampling the residual does not keep decreasing to an arbitrary small level through the iterative procedure. For this, we use the simplified 1D model and code described above. That way we do not get hampered by the complexity of the B2-EIRENE code. We investigate why the residual often can not reach machine precision (convergence to machine precision is not required in practice, but we are interested in the underlying reason).

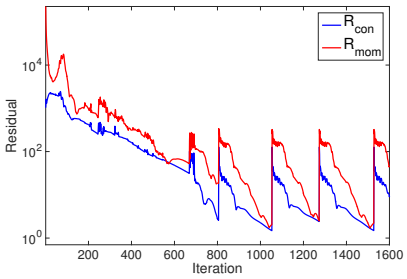

(a) Test simulation 1

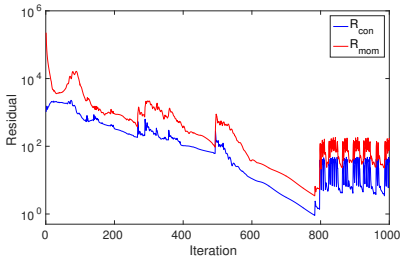

(b) Test simulation 2

Fig. 3: The blue and red line are the global residuals of the discretized continuity and momentum equations for the plasma.

[8] See ref. [5] how to sample from a truncated Maxwellian distribution.

We performed 100 test simulations[9] using correlated sampling. For 33 of the 100 test runs, the residuals of the plasma equations do not reach machine precision. We observed that with the failed test runs, the neutral particle trajectories could not converge to a fixed (iteration independent) state. For two of our failed test simulations, we visualize the evolution of the particle trajectories to determine the cause of the problem. In figure 3 the global residual progression is shown for these two test runs. The local residuals of the discretized plasma equations are summed and rescaled to obtain a global residual value for both the continuity and momentum equation. The convergence process, represented by the residuals at figure 3, is interrupted multiple times. When analyzing the plasma quantities and neutral quantities at every iteration, we notice that the neutral quantities (MC result) in the iteration before the rise in residual, change drastically. This means that at least one neutral path undergoes a very large change. When studying every neutral path individually, we see indeed that there is one trajectory that modifies radically during this critical iteration. For the first test run, this change in neutral particle trajectory is shown in the figure 4. At one specific collision moment in figure 4, the paths $t \mapsto X(t)$ and weight functions $t \mapsto W(t)$ in both iterations start to decorrelate from each other. In figure 5 we zoomed in at that critical point in time. In the two consecutive iterations the position of the crucial collision moves only a little bit. But this small change implies that the collision in the second iteration happens in another grid cell. The new velocity and the reduction of the weight after the collision are both strongly affected when the collision switches to another grid cell. This is caused by the piecewise constant plasma profile that is used when sampling velocities and adjusting the weights. The discontinuities of the plasma quantities at the cell faces cause huge modifications on the Maxwell distribution parameters and on the weight adjustment parameters. Consequently, the correction on the neutral quantities and its related mass, momentum and energy sources for the plasma, are also large and this causes the increased residual. For the second test run we come to the same conclusion when looking at figure 6 and figure 7.

We propose to solve this problem by making the plasma profile continuous when sampling velocities and adjusting weights. We suggest to use linear interpolation instead of nearest-neighbor interpolation, to fill the gaps between the discrete mesh points where the plasma quantities are computed. With the piecewise linear plasma profile instead of the piecewise constant profile, we get rid of the discontinuities at the cell faces that obstruct the neutral trajectories from converging to a fixed state. Repeating the 100 test simulations with the piecewise linear plasma profile, produces better results (see figure 8). Instead of 33 failed test runs, now only 3 test simulations fail to attain machine precision. Hence in most cases the originally discontinuous plasma profile caused the convergence problems.

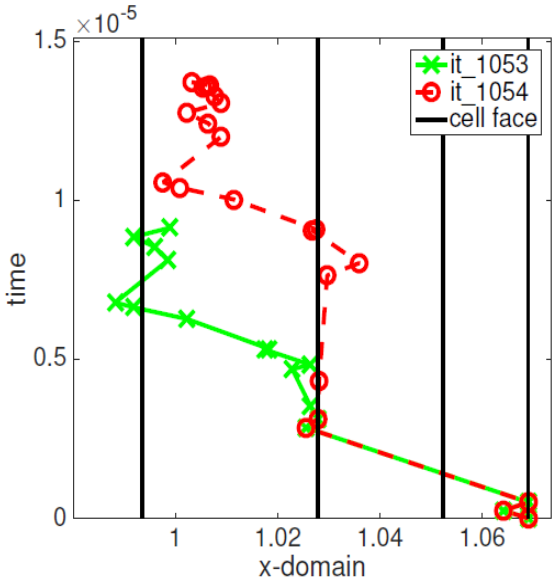

(a) The path $t \mapsto X(t)$ and the cell faces of the FV grid. The markers indicate collisions.

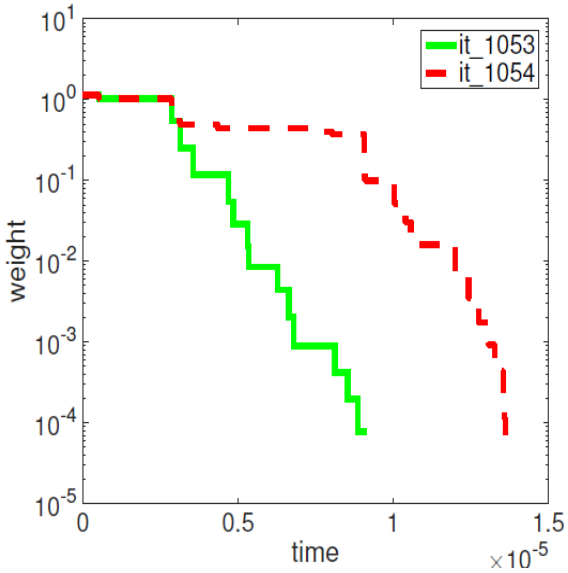

(b) The weight $t \mapsto W(t)$ (non-analog simulation).

Fig. 4: Test simulation 1: the critical neutral path in the two crucial consecutive iterations.

[9] In every test simulation we used 12 grid cells and 10 particles. Every test simulation uses its own seed for the random number generator.

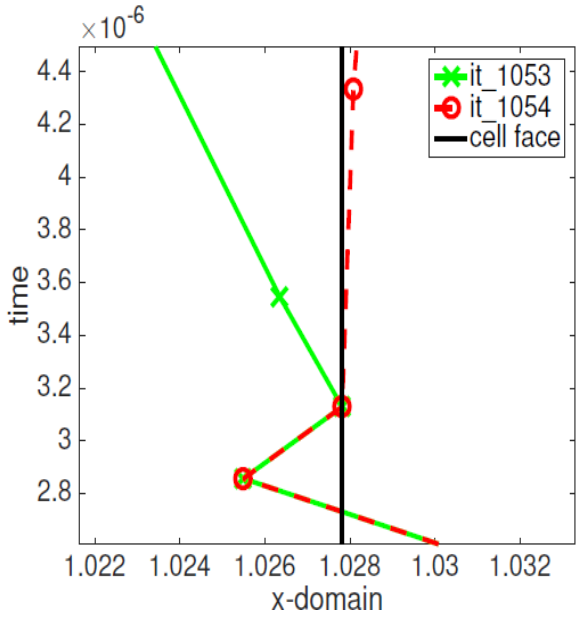

(a) Zoomed in

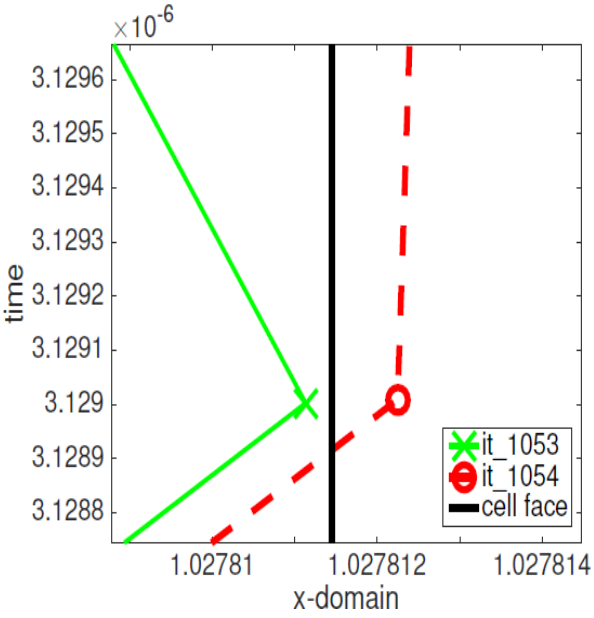

(b) Zoomed in very deep

Fig. 5: Test simulation 1: the critical neutral path in the two crucial consecutive iterations. The markers indicate collisions. We zoomed in on the critical region of the path $t \mapsto X(t)$.

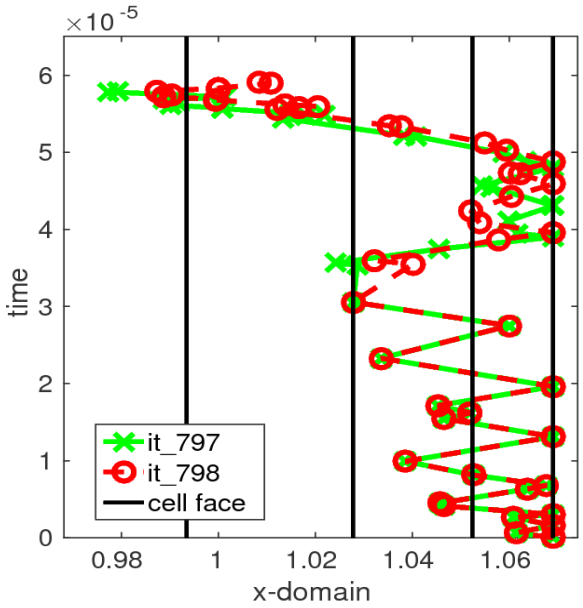

(a) The path $t \mapsto X(t)$ and the cell faces of the FV grid. The markers indicate collisions.

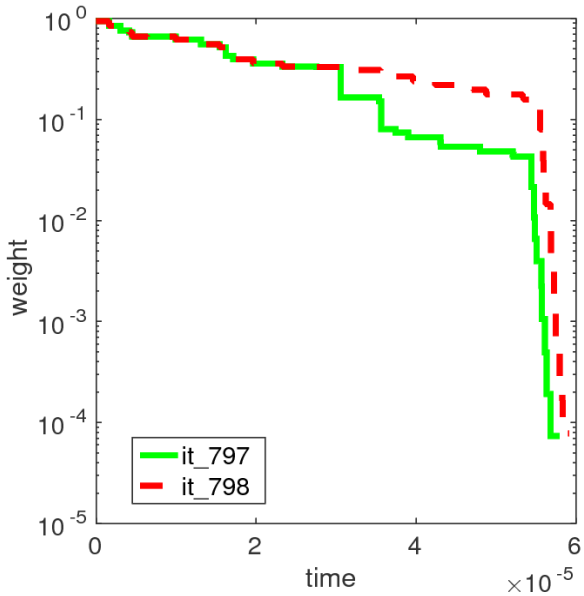

(b) The weight $t \mapsto W(t)$ (non-analog simulation).

Fig. 6: Test simulation 2: the critical neutral path in the two crucial consecutive iterations.

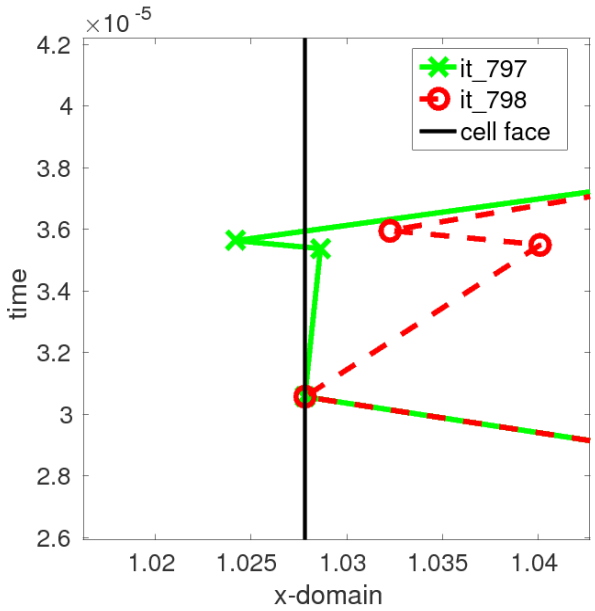

(a) Zoomed in

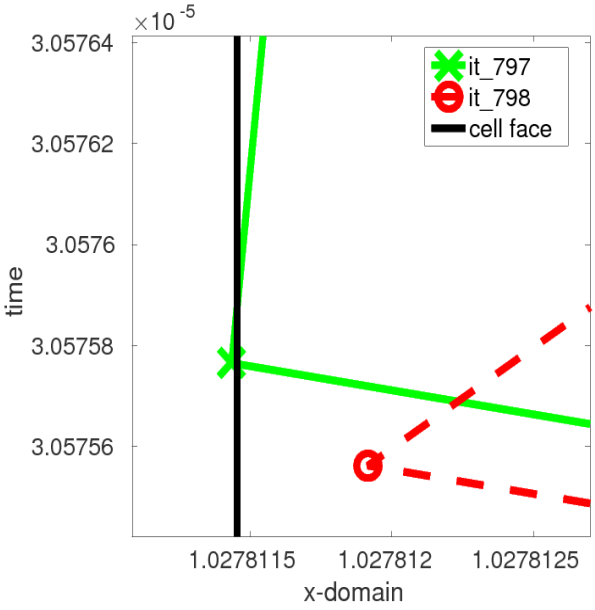

(b) Zoomed in very deep

Fig. 7: Test simulation 2: the critical neutral path in the two crucial consecutive iterations. The markers indicate collisions. We zoomed in on the critical region of the path $t \mapsto X(t)$.

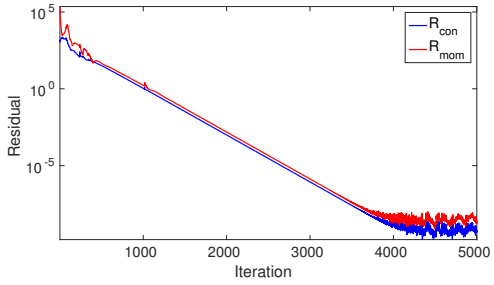

(a) Test simulation 1

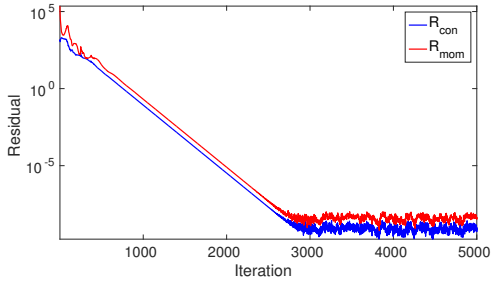

(b) Test simulation 2

Fig. 8: The blue and red line are the global residuals of the discretized continuity and momentum equations for the plasma. A piecewise linear plasma profile is used. The residuals reach machine precision.

VI. SAMPLING INTERCOLLISION TIMES FOR NEUTRAL PARTICLES

With the modifications, proposed in the previous section, for sampling velocities and adjusting weights, there are still 3 out of 100 test runs that do not converge to machine precision. For one of the three remaining test runs, the problem is due to the piecewise constant plasma profile that is still used when sampling intercollision times for neutral particle trajectories. We will again demonstrate this using a visualization of the particle paths for this specific test run. At figure 9 the critical neutral path is shown. We see a particle that crosses the cell face with a very slow speed (visible due to the steepness of the line at that point). The intercollision time changes strongly from one iteration to the next and hence the length of the trajectory also varies strongly. This causes large changes in the neutral quantity estimates, which prevents the residual from further decreasing. The sampled intercollision time varies at the cell face because a plasma profile is used that is discontinuous at the cell faces.

The piecewise constant plasma profile is used to reduce the cumulative distribution function $F_c(\tau)$ of the intercollision time τ to (22) which is then used to sample the intercollision times. A piecewise linear plasma profile using interpolation can again be the solution for the convergence problem shown at figure 9. Then we have to derive a similar expression as in (22), but for a piecewise linear profile. With linear interpolation

$F_c(\tau)$ reduces now to

$$F_c(\tau) = 1 - \prod_{j=0}^{J} \exp\Big(- \frac{R_{\text{tot}}^{j} + R_{\text{tot}}^{j+1}}{2} \Delta\tau_j \Big), \qquad (23)$$

with $\Delta\tau_j$ the time for moving from the j-th to the $(j+1)$-th encountered cell center. Remark that in (23) with R_{tot}^{0} and R_{tot}^{k+1} we do not mean the known values at the cell centers but the interpolated values at the start and end of the intercollision phase. When using (23) instead of (22) in our simulation code, the residual of the test run reaches machine precision.

VII. BOUNDARY CONDITIONS USED IN THE MONTE CARLO SIMULATION

In the two non-converging cases left, the boundary conditions for the neutral transport equation (11) were found to be the cause. When a particle hits the domain boundary, it is reflected and the weight is multiplied with the probability of non-absorption. We again analyze a failed run (see figure 10) to understand the problem related to the boundary condition. In figure 10, the fact that the particle will or will not reflect at the domain boundary has a relatively large influence on the weight reduction. Hence, if a collision occurs really close to the domain boundary, a small correction on the plasma state in the next iteration can result in a collision just after being reflected. The weight function $t \mapsto W(t)$ is really sensitive to changes in the plasma state for the specific set of used pseudorandom numbers. The boundary condition can also be interpreted as a discontinuity problem.

We propose an adjusted boundary condition to solve this problem. By reducing the weight also for collisions close to the domain boundary, we remove the discontinuity. To this end, an additional numerical parameter, i.e. the thickness L_b of the impacted region in front of the boundary, is introduced. The original and new boundary condition at the target is visualized in figure 11. In this figure the discontinuity in the original boundary condition becomes more clear.

With the use of the new boundary condition, the two runs that initially failed now converge as well. This solution is not ideal because we simulate a process that not exactly represents the physical process anymore. Consequently this artificial adjustment of the weight close to the boundary will introduce a small bias in the estimated neutral quantities. We did not further study this adverse effect.

VIII. CONCLUSIONS AND FUTURE PROSPECTS

We studied the convergence problems with correlated sampling using a simplified 1D model of the plasma and neutral transport in the divertor region of a fusion reactor. We found that in our simplified 1D code almost all convergence problems with correlated sampling are caused by the use of discontinuous plasma profile assumptions during the MC simulation. Using linear interpolation instead of nearest-neighbor interpolation for the plasma profile, overcomes these problems. Occasionally, the boundary conditions of the neutral transport equation also prevents convergence. We proposed a gradual weight reduction in front of the boundary in order to avoid this

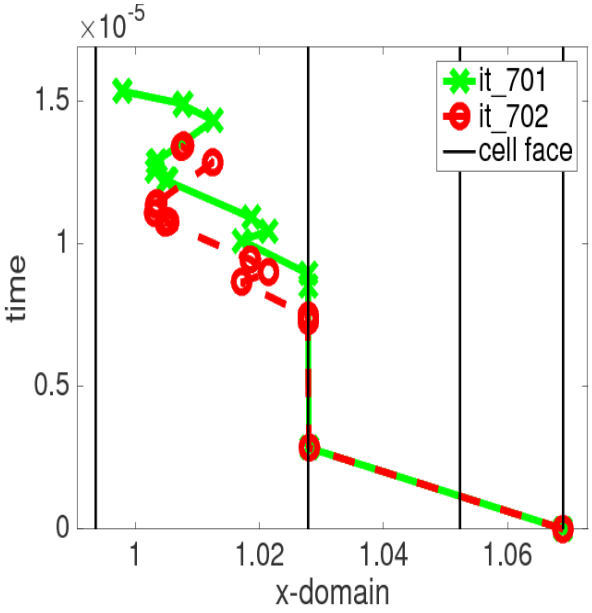

(a) The path $t \mapsto X(t)$ and the cell faces of the FV grid. The markers indicate collisions.

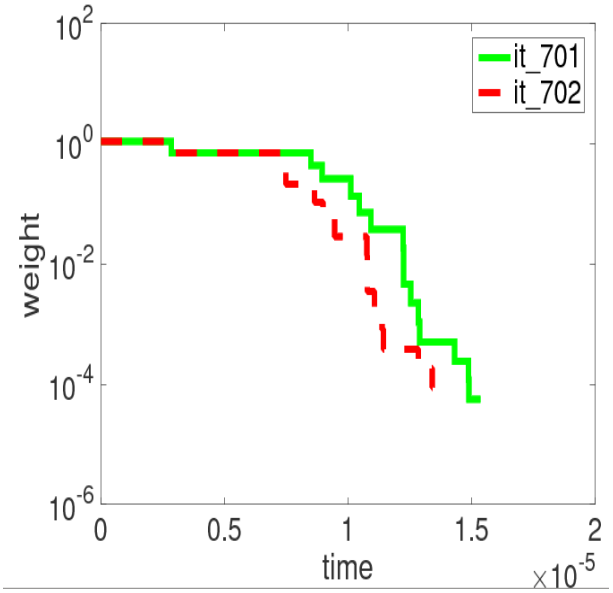

(b) The weight $t \mapsto W(t)$ (non-analog simulation).

Fig. 9: Test simulation 3: the critical neutral path in the two crucial consecutive iterations.

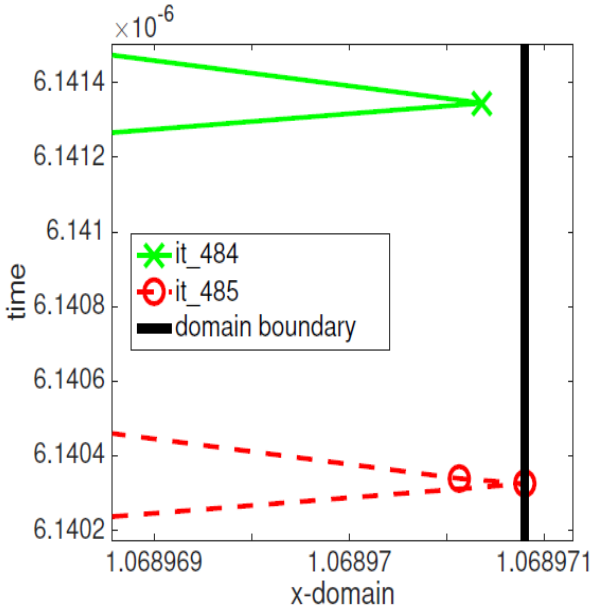

(a) the path $t \mapsto X(t)$ and one of the two boundaries of the domain. The markers indicate collisions or reflections.

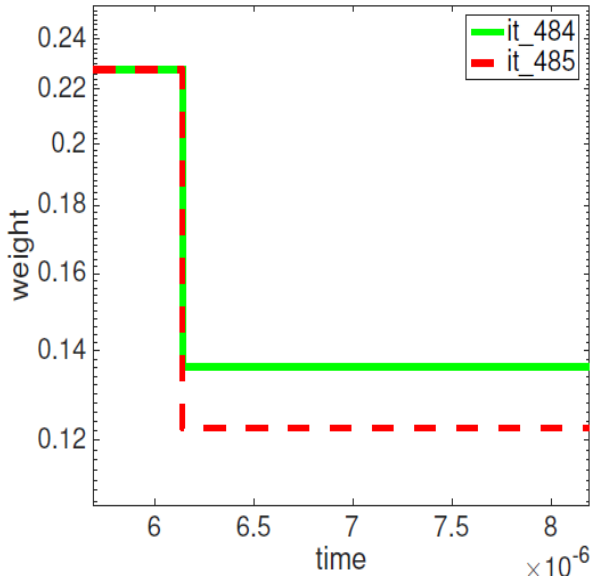

(b) The weight $t \mapsto W(t)$ (non-analog simulation).

Fig. 10: Test simulation 4: the critical neutral path in two crucial consecutive iterations. At both figures we zoomed in on the critical region.

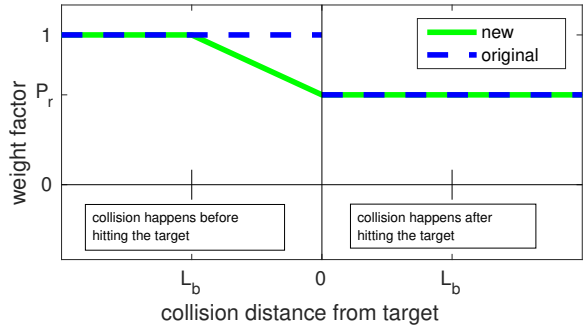

Fig. 11: Visualization of the original and proposed boundary condition at the target. The weight reduction factor due to the boundary condition is plotted as a function of the distance between the collision point and the target. The probability of reflection at the target is denoted by P_r.

problem. However, this is not an ideal solution as it introduces a bias. With these algorithm adjustments we executed 150 additional runs and they all converged to machine precision. Hence we have reason to believe that we have eliminated all convergence issues with correlated sampling for our simplified 1D code. We anticipate that the convergence issues with correlated sampling with a more complex code, such as B2-EIRENE, can also be solved by removing the discontinuities in the plasma profile and in the boundary conditions. For the 2D grid used in the B2-EIRENE code, we suggest to use bilinear interpolation.

We proposed modifications within the MC method to improve the plasma edge simulations by solving correlated sampling convergence issues. Remark that these modifications are also useful for the simulation of other coupled continuum-kinetic models that arise in other application areas.

IX. ACKNOWLEDGMENTS

This research is done during the master's thesis [11] of MB at the KU Leuven. This work has been carried out within the framework of the EUROfusion Consortium and has received funding from the Euratom research and training programme 2014-2018 under grant agreement No.633053. The views and opinions expressed herein do not necessarily reflect those of the European Commission. This research is partially funded by KU Leuven under research grant OT/13/066. BM is funded by a PhD fellowship of the Research Foundation - Flanders.

REFERENCES

1. V. KOTOV, D. REITER, and A. S. KUKUSHKIN, "Numerical study of the ITER divertor plasma with the B2-EIRENE code package," (2007).
2. D. REITER, M. BAELMANS, and P. BORNER, "The Eirene and B2-Eirene codes," *Fusion Science and Technology*, **47**, 172–186 (2005).
3. P. C. STANGEBY, "The Plasma Boundary of Magnetic Fusion Devices," *Institute of Physics Publishing* (2000).
4. W. DEKEYSER, *Optimal Plasma Edge Configurations*

for Next-Step Fusion Reactors, Ph.D. thesis, KU Leuven (2014).
5. D. REITER, "The EIRENE code user manual," (2009).
6. S. I. BRAGINSKII, "Transport processes in a plasma," *Reviews of Plasma Physics*, **1**, 205–311 (1965).
7. K. GHOOS, *The effect of noise on the convergence of the coupled B2-Eirene code system*, Master's thesis, KU Leuven (2013).
8. E. HAIRER and G. WANNER, *Solving Ordinary Differential Equations II Stiff and Differential-Algebraic Problems*, vol. 14, Springer (1996).
9. C. T. KELLEY and D. E. KEYES, "Convergence analysis of pseudo-transient continuation," *SIAM Journal on Numerical Analysis*, **35**, *2*, 508–523 (April 1998).
10. J. SPANIER and E. M. GELBARD, *Monte Carlo Principles and Neutron Transport Problems*, Addison-Welsey Series in Computer Science and Information Processing, Addison-Wesley Publishing Company (1969).
11. M. BAETEN, *Verbeterde gecorreleerde stochastische paden voor de simulatie van de plasmarand in een kernfusiereactor*, Master's thesis, KU Leuven (2016).